The mechanism of low blue light-induced leaf senescence mediated by GmCRY1s in soybean

Zhuang Li[1,2], Xiangguang Lyu[1,2], Hongyu Li[1,2], Qichao Tu[1]

dephosphorylation and accumulation of phytochrome-interacting factors (PIFs), and ultimately inducing premature leaf senescence[16–18]. In *Arabidopsis thaliana*, the absence of the *PIF* genes significantly delayed leaf senescence, whereas overexpression of *PIF* genes accelerated both age-dependent and dark-induced senescence[19]. PIFs also function in the signaling pathways of the senescence-promoting hormones, including ethylene and abscisic acid, by directly activating the expression of *ETHYLENE-INSENSITIVE 3* (*EIN3*), *ENHANCED EM LEVEL* (*EEL*), and *ABA INSENSITIVE 5* (*ABI5*)[20]. These genes directly activate the expression of the major senescence-promoting NAC transcription factor (TF) *ORESARA1* and chlorophyll degradation regulatory gene *NON-YELLOWING1* (*NYE1*), and repress the chloroplast activity maintainer gene *GOLDEN 2-LIKE2* (*GLK2*) by binding to their promoter regions[21,22].

Phytohormones are the most critical endogenous components known to control the progression of leaf senescence in plants[1,6,23]. Among them, cytokinin and auxin inhibit leaf senescence, while ethylene, salicylic acid (SA), abscisic acid (ABA), and jasmonate (JA) accelerate its aging[24–27]. However, the role of gibberellin (GA) in leaf senescence is uncertain. GA is vital for many developmental processes in plants, such as seed germination, stem elongation, and floral transition[28]. GA signaling is detected and transduced by the GA-GID1 (GIBBERELLIN INSENSITIVE DWARF1)-DELLA regulatory module. DELLA proteins, including GA INSENSITIVE (GAI), REPRESSOR OF ga1-3 (RGA), RGA-LIKE 1 (RGL1), RGL2, and RGL3, are negative regulators of GA signaling and have distinct and overlapping roles in *Arabidopsis*[29–31]. Studies have demonstrated that DELLA protein RGA interacts with WRKY6 and negatively regulates dark-induced leaf senescence and chlorophyll degradation[32,33]. RGL1 also functions as a negative regulator of leaf senescence, repressing the transcriptional activation activity of WRKY45 on several senescence-associated genes (*SAGs*), including *SAG12*, *SAG13*, *SAG113*, and *SEN4*[34]. However, the role of DELLA proteins in regulating leaf senescence in other species and whether DELLA proteins are involved in regulating light-mediated leaf senescence remain unknown.

Studies have established the roles of WRKY transcription factors (TFs) in regulating biotic and abiotic stress responses, as well as multiple developmental and physiological processes[35–37]. In *Arabidopsis*, WRKYs have been identified as important regulators of leaf senescence. For example, WRKY6 is known to positively regulate leaf senescence by specifically activating the expression of *senescence-induced receptor-like kinase* (*SIRK*) gene[38]. Meanwhile, WRKY75 has been shown to accelerate the progression of leaf senescence by promoting the transcription of *SA INDUCTION-DEFICIENT2* (*SID2*) to increase SA content and inhibiting the transcription of *CATALASE2* (*CAT2*) to reduce H_2O_2 scavenging[39]. WRKY28 also plays a role in high R:FR-induced leaf senescence. FHY3, the key regulator of the phytochrome A-mediated signaling pathway, directly binds to the promoter region of *WRKY28* to suppress its expression under high R:FR light conditions, thereby negatively regulating SA biosynthesis and leaf senescence[40].

In contrast to the well-documented mechanism of low R:FR-induced leaf senescence in the model plant *Arabidopsis*, the physiological process of LBL-induced leaf senescence remains poorly understood. CRYs, as the primary blue-light receptors play essential roles in photomorphogenesis and photoperiodic flowering[8,41,42], appear to have no apparent influence on leaf senescence in *Arabidopsis*[21]. A study on soybean revealed that GmCRY2a negatively regulates leaf senescence by interacting with the basic helix-loop-helix transcriptional factor GmCIB1 (cryptochrome-interacting bHLH1) and inhibiting its transcriptional activity on *SAGs*[43]. Additionally, LBL induces obvious SAS including exaggerated stem elongation in soybean[44], suggesting that soybean may be a suitable organism to study the mechanisms of LBL-induced leaf senescence in plants.

In this study, we demonstrate that LBL can induce clear leaf senescence in soybean. We find that, under normal light conditions, GmCRY1s interact with and stabilize the DELLA proteins

nd it on

p
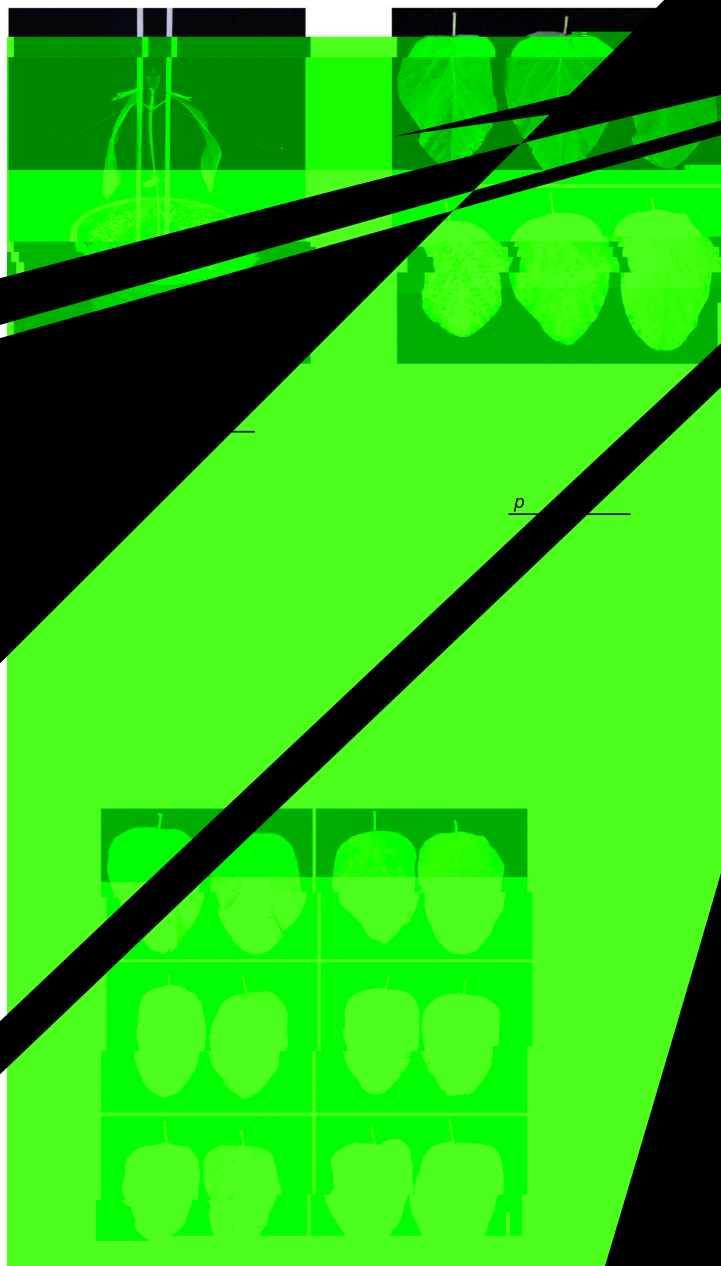
To assess the role of GmCRYs in LBL-induced leaf senescence, compared the performance of the *Gmcry1s-qm* and *Gmcr* mutants under these conditions. Our findings revealed tha induced leaf senescence was significantly disrupted by mutations and slightly impaired by *Gmcry2s* mutations (Fi indicating that GmCRY1s are dominantly responsible for LB

Fig. 1 | Phenotypic analysis of LBL-induced leaf senescence in the wild-type TL1 and *Gmcry* mutants. a Experimental scheme for LBL treatment. For a pair of uni-foliate leaves, one was covered with two layers of yellow filter to imitate the LBL condition, and the other one was covered with two layers of transparent filters as the control. White and yellow arrows indicate the transparent and yellow filters, respectively. **b** Leaf senescence phenotypes of wild-type TL1 cultivar induced by LBL treatment. Seedlings were de-etiolated under continuous white light for 10 days, then a pair of unifoliate leaves were treated with different light regimes (LBL or WL) for 14 days as in (**a**). Scale bar, 5 cm. **c** Chlorophyll content in the leaves as in (**b**). Values are means ± SD (*n* = 5 biological replicates). **d** Relative transcript levels of senescence-associated genes *GmSAG12*, *GmSAG13*, and *GmSAG113* in the leaves as in

(**b**). Values are means ± SD (*n* = 3 biological replicates). The *GmActin* gene was used as the internal control. **e** Leaf senescence phenotypes of indicated lines treated by WL and LBL as in (**b**). Scale bar, 3 cm. **f** Chlorophyll content in the leaves as in (**e**). The percentage decrease in chlorophyll content under WL compared to LBL is indicated by the values above the respective *p* values. Values are means ± SD (*n* = 5 biological replicates). **g** Relative transcript levels of senescence-associated genes in the indicated lines in response to LBL treatment as in (**b**). The unifoliate leaves were collected for RT-qPCR analysis. Values are means ± SD (*n* = 3 biological replicates). The *GmActin* gene was used as the internal control. All above *P* values were calculated by unpaired two-tailed *t*-test. Source data are provided as a Source Data file.

GmCRY1b interacts with DELLA proteins RGAa and RGAb in response to blue light

To elucidate the molecular mechanism via which GmCRY1s repress leaf senescence, we used a yeast two-hybrid (Y2H) system to identify its potential interaction partners. Considering the strong autoactivation ability of GmCRY1b, the C-terminal truncated form of GmCRY1b (GmCCT1b-33aa) was fused with the BD domain of the pBridge vector to obtain the bait for yeast hybrid screening (Fig. 2a). The yeast cells harboring the bait were transformed with a library of prey protein-encoding cDNAs fused to GAL4-AD. The screening discovered eight putative interacting partners of GmCRY1b (Supplementary Data 2), including a DELLA protein GmRGAa (Glyma.05G140400), which has a paralogous protein GmRGAb (Glyma.08G095800, with 95.4% similarity to GmRGAa) in soybean (Supplementary Fig. 9). Further, the open reading frames (ORF) of GmRGAa and GmRGAb in soybean were fused to the AD domain of the pGADT7 vector and used for further inter-action experiments with various truncated versions of GmCRY1b. The bait and prey vectors were co-transformed into yeast, and the protein-protein interactions were reconstructed. The two-hybrid screening demonstrated that a region of 33 amino acids (451-483) in the middle part of GmCRY1b is essential to interact with the DELLA proteins physically (Fig. 2b, c, and Supplementary Fig. 10). To determine the motif of DELLA protein that interacts with GmCRY1b, we used trun-cated forms of GmRGAa (N-terminal and C-terminal) for Y2H experi-ments. Our results showed that the N-terminal truncated form of GmRGAa caused strong auto-activation in yeast, whereas the C-terminal truncated form of GmRGAa physically interacted with GmCRY1b, as shown in Supplementary Fig. 11.

We further investigated the interaction between GmCRY1b and DELLA proteins in plant cells by infiltrating *Agrobacterium* expressing indicated proteins into soybean leaves[48]. The results revealed that GmCRY1b interacted with GmRGAa and GmRGAb in a blue light-dependent manner, as evidenced by the co-immunoprecipitation (Co-IP) assay (Fig. 2d). This blue light-dependent interaction between GmCRY1b and DELLA proteins was further corroborated using the bimolecular fluorescence complementation (BiFC) assay in soybean mesophyll protoplasts (Fig. 2e, Supplementary Fig. 12), and a split-LUC assay in *Nicotiana benthamiana* leaves (Supplementary Fig. 13), with the interaction being abrogated under LBL conditions. The BiFC sig-nals were observed mainly in the nucleus, which is consistent with the subcellular localization results that showed GmCRY1b occupies the same location as DELLA proteins in the nucleus (Supplementary Fig. 14), suggesting a function of the GmCRY1b-GmDELLA complex in the nucleus.

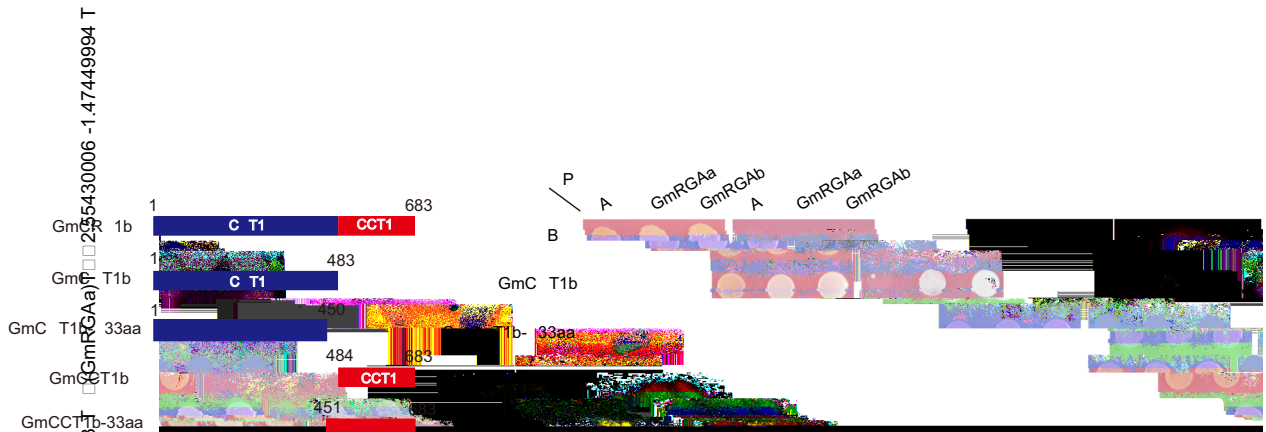## Photoactivated GmCRY1b inhibits the degradation of RGAa and RGAb

Based on the knowledge that DELLA proteins act as central repressors in gibberellin (GA) signaling pathway[31], we tested if GA acts as a senescence-associated hormone in soybean. We conducted experi-ments using GA$_3$ or PAC (paclobutrazol) treatment on seedlings, and our results showed that GA$_3$ accelerated leaf senescence, while PAC

delayed it, with higher chlorophyll content and lower senescence index (Supplementary Fig. 15). Furthermore, overexpression of *GmGA2ox-7a*, which deactivates bioactive GAs[44], also show delayed senescence (Supplementary Fig. 16), indicating that GA is a senescence-promoting hormone in soybean.
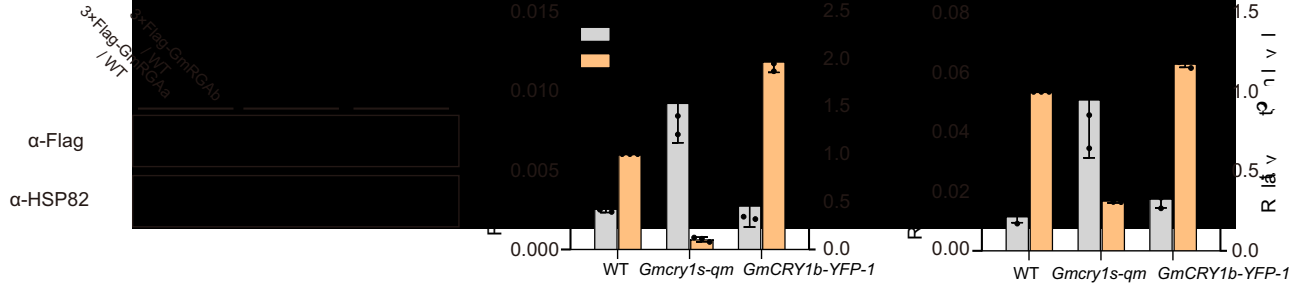
We then investigated the role of GmCRY1s in GA-mediated leaf senescence and found that GA could induce significant senescence in *Gmcry1s-qm* mutant (Supplementary Fig. 17), suggesting that GmCRY1s inhibit GA-mediated leaf senescence in soybean. Given that GA pro-motes the degradation of DELLA proteins, we hypothesized that binding of GmCRY1b to DELLA proteins could impede access of the GA receptor GID1 to DELLA proteins, thus interfering with DELLA degradation. To test this possibility, we used the RICE system to compare the protein levels of GmRGAa and GmRGAb in the *Gmcry1s-qm* mutant, *GmCRY1b-OE* line and wild type under continuous light or after LBL treatment. The immunoblot results revealed that GmRGAa and GmRGAb proteins in the wild-type callus were gradually reduced under LBL conditions at 3, 5, and 8 h, while the proteins remained constant under continuous white light (Supplementary Fig. 18). Consistent with the results observed in soybean hairy root callus, GmRGAb protein also showed a similar reduction in response to LBL in the *Flag-GmRGAb-1* stable transgenic line (Fig. 2f, g). Moreover, the GmRGAa and GmRGAb protein levels were significantly lower in the *Gmcry1s-qm* mutant but markedly higher in the *GmCRY1b* overexpressing line in comparison to the wild type (Fig. 2h–j). These results demonstrate that GmCRY1b stabilizes GmRGAa and GmRGAb in a blue light-dependent manner and releases the degradation of GmRGAa and GmRGAb in response to LBL.

GmRGAa and GmRGAb negatively regulate LBL-induced leaf senescence

To determine the roles of DELLA proteins in regulating soybean leaf senescence, we knocked out the *GmRGAa* and *GmRGAb* genes using CRISPR-Cas9 technology. Multiple mutants were identified for each gene, including *Gmrgaa-1*, *Gmrgab-1*, and *Gmrgab-2* (Supplementary Fig. 19) with mutations creating premature stop codons in the targeted genes (Supplementary Fig. 20). We then crossed *Gmrgaa-1* with *Gmrgab-1* to obtain the *Gmrgaa Gmrgab* double (*Gmrgas-dm*) mutant. Although the *Gmrgaa-1*, *Gmrgab-1*, and *Gmrgab-2* single mutants did not exhibit an obvious senescence phenotype, the *Gmrgas-dm* mutant displayed a significantly precocious leaf senescence with lower chlor-ophyll content, higher cotyledon and leaf senescence index, and higher expression levels of *SAGs* compared to the wild type (Supple-mentary Fig. 21). Additionally, two *GmRGAb* overexpression lines (*GmRGAb-OE-1* and *GmRGAb-OE-2*) harboring the *GmRGAb* coding sequence driven by the 35S promoter were generated (Supplementary Fig. 22). Compared to the wild type, the *Gmrgas-dm* mutant presented premature leaf senescence, while the *GmRGAb-OE* lines showed delayed leaf senescence under natural field conditions (Supplemen-tary Fig. 23), indicating that GmRGAa and GmRGAb play a negative role in leaf senescence. We further analyzed the agronomic traits of transgenic lines lacking or overexpressing *GmRGAs* at the R8 stage under natural field conditions. Our results demonstrated that the main

GmCR 1b   1   C T1   CCT1   683

GmC T1b   1   C T1   483

GmC T1b-33aa   1   C T1   450

GmCCT1b   484   CCT1   683

GmCCT1b-33aa   451

P A   GmRGAa   GmRGAb   A   GmRGAa   GmRGAb

B

GmC T1b

T1b- 33aa

h

3×Flag-GmRGAb / WT

3×Flag-GmRGAa / WT

α-Flag

α-HSP82

WT   *Gmcry1s-qm*   *GmCRY1b-YFP-1*

WT   *Gmcry1s-qm*   *GmCRY1b-YFP-1*

yield traits, such as node number, branch number, and total grain weight per plant, did not exhibit any significant change among each line (Supplementary Fig. 24).

To investigate the role of GmRGAa and GmRGAb in LBL-induced leaf senescence, we grew *Gmrgaa-1*, *Gmrgab-1* and *Gmrgas-dm* seedlings for LBL treatment (Supplementary Fig. 25a). Phenotypic analysis revealed that the reduction in chlorophyll content induced by LBL was gradually reduced in the *Gmrgaa-1*, *Gmrgab-1*, and *Gmrgas-dm* mutants compared to the wild type (Supplementary Fig. 25b). This, coupled with the fact that LBL promotes the degradation of GmRGAa and GmRGAb, suggests that LBL triggers leaf senescence at least par-

genes (DEGs) among the wild type, *Gmcry1s-qm* and *GmCRY1b-OE* lines. We previously identified 3055 and 638 DEGs in the *Gmcry1s-qm* mutant and the *GmCRY1b-OE* line, respectively, compared to the wild type[44]. Among these, 249 genes exhibited opposite expression patterns in the *Gmcry1s-qm* mutant and *GmCRY1b-OE* line compared to wild type. We identified 14 senescence-related genes encoding WRKY TFs, MYB TFs, SEN4, cysteine protease, and B-BOX domain proteins that might

regulate leaf senescence in soybean (Supplementary Data 3). Among these, *Glyma.06G168400*, encoding a typical WRKY TF named GmWRKY100 in a previous study[49] (Supplementary Fig. 27a), exhibited significantly down-regulated expression in the *GmCRY1b-OE* line and up-regulated expression in the *Gmcry1s-qm* mutant (Fig. 4a, b), suggesting that GmWRKY100 may play a role in GmCRY1s-mediated regulation of leaf senescence.

b
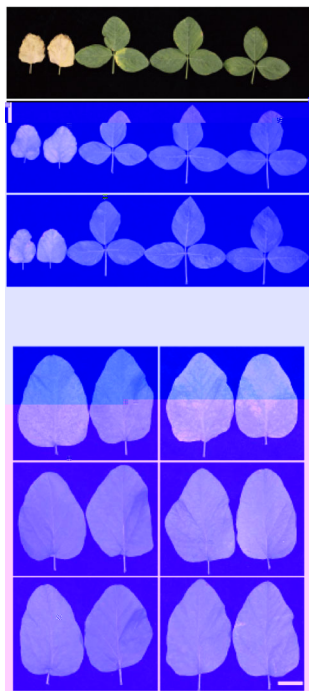
The transcriptional level of *GmWRKY100* was observed to increase in association with the onset of leaf senescence (Fig. 4c), suggesting that *GmWRKY100* promotes leaf senescence in soybean. Notably, the expression levels of *GmCRY1b*, *GmRGAa* and *GmRGAb* also increased as leaf senescence progressed (Supplementary Fig. 28), suggesting the existence of negative feedback regulation among GmCRY1s, DELLAs, and GmWRKY100 in the process of leaf senescence. To test this, we generated *GmWRKY100* knockout mutants using the CRISPR/Cas9-engineered genome-editing approach. We identified two independent mutants, *Gmwrky100-1* and *Gmwrky100-7*, with 2 bp and 5 bp deletions, respectively, which caused frame-shift mutations and premature stop codons (Supplementary Fig. 27b, c). Compared with the wild type, these mutants showed delayed leaf senescence under green-house and natural field conditions (Fig. 4d, Supplementary Fig. 29), with slower chlorophyll degradation (Fig. 4e), lower cotyledon and leaf senescence index (Supplementary Fig. 30), and lower expression levels of *GmSAG12* (Fig. 4f). LBL treatment significantly induced the expression of *GmWRKY100*, whereas its expression remained constant under continuous white light (Supplementary Fig. 31). To determine the function of GmWRKY100 in LBL-induced leaf senescence, we grew wild-type plants and *Gmwrky100* mutants under WL and LBL conditions, respectively. Phenotypic analysis revealed a reduced LBL-induced leaf senescence in the *Gmwrky100* mutant compared to the wild type (Fig. 4g, Supplementary Fig. 32). The statistical analysis of two-way ANOVA indicated a significant interaction between genotypes and light treatments in terms of chlorophyll content and senescence marker gene *GmSAG13* (Fig. 4h, i). These results suggest that the *GmWRKY100* gene plays a significant role in LBL-induced leaf senescence.

LBL releases the inhibitory effect of DELLA proteins on *GmWRKY100* transcription

Given the fact that *GmRGAa* and *GmRGAb* delay leaf senescence, while *GmWRKY100* promotes it, we surmise that *GmWRKY100* transcription may be negatively regulated by GmRGAa and GmRGAb. This is supported by the observation that the mRNA level of *GmWRKY100* was upregulated by more than 20-fold in *Gmrgas-dm* mutants compared to wild type (Fig. 5

a
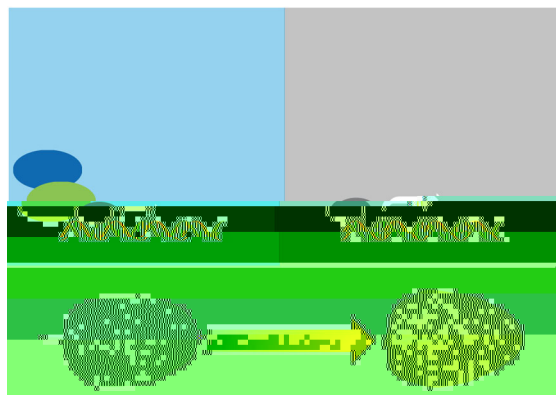
(*Glyma.11G144900*), *GmSAG13* (*Glyma.12G059200*), *GmSAG113* (*Glyma.14G066400*), *GmGA2ox7a* (*Glyma.20G141200*), and *GmActin* (*Glyma.18G290800*).

To construct the overexpression plant transformation vectors, the coding DNA sequence (CDS) of each indicated gene was amplified by PCR using cDNA derived from young leaves of Williams 82 seedlings, cloned into the gateway entry vector pDONR-Zeo by BP reaction, and then further cloned into the destination binary overexpression vector pEarleyGate101 or pEarleyGate104 by LR reaction using the Gateway recombination system (Invitrogen) following the manufacturer's instructions[61]. To generate the CRISPR-Cas9-engineered mutants, gRNAs were designed using the web tool CRISPRdirect (http://crispr.dbcls.jp/)[62]. The efficiency of each candidate gRNA was estimated using the soybean hairy root system[63], and efficient candidates were selected for soybean transformation. The above expression plasmids were individually introduced into *Agrobacterium tumefaciens* strain EHA105 via electroporation and then transformed into wild-type soybean (Tian-Long 1) by *agrobacterium*-mediated cotyledonary node transformation system[64]. Briefly, healthy seeds were selected and sterilized by chlorine for 18 h, then soaked into sterilized water overnight for imbibition. The seed coat was gently removed, and the swelled seeds were cut in half. The cotyledon explants were gently scratched at the cotyledon node and were immersed in *Agrobacterium* (EHA105) which harbors expression vectors for 30 min for infection. The infected explants were transferred to the co-cultured medium and subjected to dark conditions for three days at 25 °C. After 3 days of co-culture, the explants were washed with sterilized water supplemented with 50 mg/L timentin, 50 mg/L vancomycin, and 100 mg/L cefotaxime to remove the bacteria on the surface, then transferred to the shoot initiation medium with the hypocotyl embedded in the medium under a 12 h light/12 h dark photoperiod at 26 °C, and subcultured once for 10 days to fresh medium with three repetitions. The explants with tufted shoots were then transferred to shoot elongation medium and subcultured once for 10 days to fresh medium with three repetitions. The elongated shoots were cut and moved to the rooting medium. The shoot initiation medium and shoot elongation medium contain phosphinothricin (5 mg/L) to screen positive transgenic shoots.

Total RNA isolation and gene expression analysis
To measure the expression of senescence-associated genes during leaf senescence, leaves of the indicated genotypes were flash-frozen in liquid nitrogen. Total RNA was extracted using TRIzol reagent (Invitrogen). The cDNA was synthesized from 2 μg of total RNA using Oligo(dT)$_{18}$ primer with TransScript II One-Step gDNA Removal and cDNA Synthesis SuperMix (TransGen). Real-time PCR instrument qTOWER 3G (analytikjena) was used for the quantitative PCR reaction following the manufacturer's instructions. Briefly, the cDNA was diluted 10-fold, and 5 μL of diluted cDNA was used as the template and amplified with Taq Pro Universal SYBR qPCR Master Mix (Vazyme) with specific primer sets (Supplementary Data 1) in a 20 μL quantitative PCR reaction, which was pre-denatured at 95 °C for 5 min, followed by a 40-cycle program (95 °C, 10 s; 60 °C, 20 s; 72 °C, 30 s per cycle). The soybean *GmActin* gene (*Glyma.18G290800*) was used as an internal control. The quantitative PCR results shown are the average (±SD) of three biological repeats. Primers used in the present study were listed in Supplementary Data 1.

Western blot
To analyze the protein expression in transgenic plants and fairy root calluses, total proteins of Tian-Long 1, and the indicated transgenic plants were extracted with protein extraction buffer (50 mM Tris-HCl pH 7.5, 150 mM NaCl, 5 mM EDTA, 0.1% Triton X-100, 0.2% NP-40,1 mM PMSF and 1 tablet/50 mL of protease inhibitor cocktail). The homogenate was clarified by centrifugation at 14,000 g for 15 min at 4 °C, and aliquots of the supernatant were combined with 4×SDS sample loading buffer and heated at 99 °C for 8 min to denature the protein. The antibody anti-FLAG (M20008L) and anti-GFP antibody (598) were obtained from Abmart and MBL, respectively.

Transient dual-luciferase reporter system
A 2.24-kb promoter sequence of *GmWRKY100* was amplified from soybean Williams 82 genomic DNA and inserted into the pGreenII 0800-LUC vector to control the luciferase (LUC) gene, which was used as reporter plasmids. The renilla luciferase (REN) gene under the control of the 35S promoter in the pGreenII 0800-LUC vector was used as an internal control[65]. The coding sequence of *GmCRY1b*, *GmRGAa*, *GmRGAb*, and GUS were amplified by PCR, inserted into the 0641-3×Flag vector, and used as an effector plasmid. 0641-GUS-3×Flag vector was set as negative effector control. Soybean mesophyll protoplasts were prepared, transfected, and cultured as described previously[66]. The ratio of LUC to REN was determined for the dual-luciferase reporter system (Promega, United States) on Centro XS^3 LB 960 after culturing the protoplasts under normal white light or LBL conditions for 4 h. Transcriptional activity of the *GmWRKY100* promoter was calculated as LUC to REN ratio of three biological replicates.

Measurement of chlorophyll content
The measurement of chlorophyll content was performed as described previously[43]. Briefly, 0.2 g of fresh sample of each indicated plant was frozen in liquid nitrogen, ground to powder, mixed thoroughly with 20 mL of 80% acetone, and stored at −20 °C for 1 h in the dark. Then the sample was centrifuged at 12,800 g for 3 min and 1 mL of supernatants was measured for absorbance at 663 nm and 645 nm. Chlorophyll concentrations were calculated using the following formulas:

$$\text{Concentration of total chlorophyll} = (20.2A_{645} + 8.02A_{663})\,\text{mg/g}$$

For the measurement of chlorophyll content in living plants, the SPAD value was scored using a SPAD meter (SPAD-502, Minolta Camera Co., Osaka, Japan) as previously described[67].

Yeast two-hybrid assay
The yeast two-hybrid assay was performed as previously described[68]. In brief, the various truncated versions of GmCRY1b, and the full-length coding sequence (CDS) of DELLA proteins GmRGAa and GmRGAb were cloned into the bait vector pBridge and the prey vector pGADT7, respectively. The plasmids were transformed into the yeast strain AH109 (Clontech), and the yeast cells were grown on a minimal medium SD/-Leu-Trp according to the manufacturer's instructions (Clontech). Positive clones were selected on SD/-Ade-His-Leu-Trp selection medium containing 1 mM 3-AT (3-amino-1,2,4-triazole). Quantitation of β-galactosidase (β-gal) activity was determined as described by the manufacturer (Clontech).

Root-induced callus expression system (RICE)
The *3×Flag-GmRGAa* and *3×Flag-GmRGAb* plasmids were introduced into *Agrobacterium tumefaciens* strain K599 via electroporation, which further infected the young seedlings of WT, *Gmcry1s-qm*, and *GmCRY1b* overexpressing line at the hypocotyl region to induce transgenic hairy roots according to previous methods with minor changes[69]. The positive transgenic hairy roots were screened in the callus induction medium (2.22 g/L Murashige & Skoog Basal Medium with Vitamins, 0.59 g/L MES monohydrate, 30 g/L sucrose, 1 mg/L 2, 4-D, 0.1 mg/L 6-BA, 0.1 g/L Timentin) contains 5 mg/L phosphinothricin (PPT). The positive transgenic calluses were cultured in the callus induction medium for 20 days under long-day (16 h of light /8 h of dark) conditions. These transgenic calluses lines were further confirmed by RT-qPCR and immunoblot analysis. Three independent hairy root calluses lines of each indicated genotype were used for transcriptional analysis and identification of protein levels.

Soybean leaf injection

The seedlings of *GmCRY1b-YFP-1* transgenic line were grown under long-day conditions (16 h light/8 h dark) for seven days. The fully expanded unifoliate leaves were wiped with a brush[48]. The *Agrobacterium* strain GV3101 transformed with 3×Flag-GmRGAa or 3×Flag-GmRGAb overexpression vectors were resuspended with infiltration buffer (10 mM MES pH 5.6, 200 μM acetosyringone) to $OD_{600} = 1$, and then pressure-infiltrated into the lower epidermis of the leaves using a vacuum pump until the leaves were completely wet. The transformed soybean seedlings were recovered under continuous darkness for one day and then grown under normal long-day conditions.

Co-immunoprecipitation assay

Soybean leaves of *GmCRY1b-YFP-1* overexpression line transiently transformed with indicated proteins by leaf injection were flash-frozen in liquid nitrogen, ground to powder, and mixed thoroughly with protein extraction buffer (50 mM Tris-HCl pH 7.5, 150 mM NaCl, 5 mM EDTA, 0.1% Triton X-100, 0.2% NP-40, 1 mM PMSF and 1 tablet/50 mL of protease inhibitor cocktail). The protein extracts were incubated at 4 °C for 30 min and centrifuged at 13,000 g for 30 min. After centrifugation, the supernatants were incubated at 4 °C with GFP-Trap Agarose (ChromoTek) for 4 h. The GFP-Trap Agarose was collected by spinning at 1500 rpm for 3 min and washed three times with the wash buffer (10 mM Tris-HCl pH = 7.5, 150 mM NaCl, 0.5 mM EDTA). The proteins were eluted from the GFP-Trap Agarose by mixing with 4×SDS-PAGE sample buffer, boiled for 8 min, and spun at 12,000 rpm for 5 min at room temperature, then subjected to immunoblot analysis. Immunoblots were performed using the anti-GFP antibody (MBL) for probing GmCRY1b-YFP and the anti-Flag antibody (Abmart) for probing Flag-GmRGAa and Flag-GmRGAb.

Multiple alignment and construction of phylogenetic tree

The protein sequences of GAI(At1g14920), RGA(At2g01570), RGL1(At1g66350), RGL2(At3g03450), RGL3(At5g17490), WRKY45(At3g01970) and WRKY75(At5g13080) were retrieved from TAIR (https://www.arabidopsis.org/index.jsp). The DELLA proteins and GmWRKY100 protein sequences of Glycine max (GmRGAa, Glyma.05G140400; GmRGAb, Glyma.08G095800; GmWRKY100, Glyma.06G168400, and their homologous gene) are available at Phytozome (https://phytozome.jgi.doe.gov/pz/portal.html). Amino acid sequences of DELLA proteins, GmWRKY100, and their homologous proteins were aligned by ClustalW in MEGA X and manually adjusted. The phylogenetic tree was constructed using the neighbor-joining method in MEGA X software[70].

Chromatin immuno-precipitation (ChIP) assay

Leaf samples were collected from 10-day-old seedlings under continuous light from Tian-Long 1, *p35S:3×Flag-GmRGAb* transgenic lines. ChIP assay was performed as previously described[71]. Briefly, 2 g leaves tissue sample was used in the ChIP experiment, samples were fixed on ice for 20 min in 1% formaldehyde under vacuum. Nuclei were isolated and sonicated. The solubilized chromatin was immunoprecipitated by anti-Flag M2 Magnetic Beads (M8823). The coimmunoprecipitated DNA was recovered and analyzed by RT-qPCR in triplicate. Relative fold enrichment was calculated by normalizing the amount of a target DNA fragment against that of a genomic fragment of a reference gene, *GmWRKY100 (Glyma.06G168400)*, and then by normalizing the value of the input DNA. The primers used for amplification are listed in (Supplementary Data 1).

Split-luciferase assay

For split-LUC assays to detect protein-protein interactions, the cDNA fragments encoding GmCRY1b, GmRGAa, and GmRGAb were cloned into pCambia1300-nLUC and pCambia1300-cLUC. These constructs expressing Venus-nLUC, cLUC-Venus, GmRGAa-nLUC, GmRGAb-nLUC, and cLUC-GmCRY1b were introduced individually into *Agrobacterium* strain GV3101. The resulting colonies harboring the indicated constructs expressing nLUC or cLUC fusions were grown in LB medium overnight, collected by centrifugation, and resuspended in infiltration buffer (10 mM MgCl₂, 10 mM MES pH 5.6, 200 μM AS (Acetosyringone)). Bacterial suspensions were then mixed in a 1:1 ratio and infiltrated into *N. benthamiana* leaves. The infiltrated *N. benthamianas* were grown under white light or LBL conditions for 2 days after 12 h darkness-treatment. Then, *N. benthamiana* leaves were infiltrated with 1 mM D-luciferin sodium salt substrate and kept in the dark for 5 min. LUC signal was collected on a luminescent imaging workstation (Tanon 5200 Chemiluminescence imaging system).

Bimolecular fluorescent complimentary (BIFC)

The CDS of GmCRY1b and DELLA proteins GmRGAa and GmRGAb were cloned into the pCCFP-GW or pNYFP-GW vector using a gateway recombination system. Soybean seedlings were grown under short-day (8 h light/16 h dark) conditions, at a light intensity of 120-180 μmol m⁻² s⁻¹ and a temperature of 26 °C. Mesophyll protoplasts were isolated from the unifoliate leaves of soybean and transformed following the reported procedure[72]. Protoplasts were transfected with the indicated plasmid DNA. Samples were incubated for 12 to 14 h in the dark at 26 °C, transferred to white light or LBL conditions for 2 h, and then analyzed under confocal microscopy (Zeiss LSM 980).

Statistics and reproducibility

Multiple comparisons were conducted using GraphPad Prism 9.5 software with one-way or two-way ANOVA and two-sided Tukey test. For comparisons between two groups, two-tailed Student's *t*-tests were performed using Microsoft Excel. The statistical test employed and the corresponding number of individuals (*n*) for each experiment were both provided in the figure legends. For the expression analysis, at least three individual plants per tissue sample were pooled, and a minimum of three RT-qPCR reactions (technical replicates) were performed for three biological replicates. All experiments were conducted at least thrice for consistency.

Reporting summary

Further information on research design is available in the Nature Portfolio Reporting Summary linked to this article.

Data availability

All the data generated in this study are provided in the Supplementary Information and Source Data file. Source data are provided with this paper.

References

1. Lim, P. O., Kim, H. J. & Nam, H. G. Leaf senescence. Annu. Rev. Plant Biol. **58**, 115–136 (2007).
2. Woo, H. R., Kim, H. J., Lim, P. O. & Nam, H. G. Leaf senescence: systems and dynamics aspects. Annu. Rev. Plant Biol. **70**, 347–376 (2019).
3. Schippers, J. H. Transcriptional networks in leaf senescence. Curr. Opin. Plant Biol. **27**, 77–83 (2015).
4. Quirino, B. F., Noh, Y. S., Himelblau, E. & Amasino, R. M. Molecular aspects of leaf senescence. Trends Plant Sci. **5**, 278–282 (2000).
5. Yoshida, S. Molecular regulation of leaf senescence. Curr. Opin. Plant Biol. **6**, 79–84 (2003).
6. Guo, Y. & Gan, S. Leaf senescence: signals, execution, and regulation. Curr. Top. Dev. Biol. **71**, 83–112 (2005).
7. Biswal, U. C. & Biswal, B. Photocontrol of leaf senescence. Photochem. Photobiol. **39**, 875–879 (1984).
8. Cashmore, A. R., Jarillo, J. A., Wu, Y. J. & Liu, D. Cryptochromes: blue light receptors for plants and animals. Science **284**, 760–765 (1999).

9. Smith, H. Phytochromes and light signal perception by plants-an emerging synthesis. Nature **407**, 585–591 (2000).

10. Briggs, W. R., Christie, J. M. & Salomon, M. Phototropins: a new family of flavin-binding blue light receptors in plants. Antioxid. Redox Signal **3**, 775–788 (2001).

11. Frohnmeyer, H. & Staiger, D. Ultraviolet-B radiation-mediated responses in plants. Balancing damage and protection. Plant Physiol. **133**, 1420–1428 (2003).

12. Zhang, M. et al. Progress in soybean functional genomics over the past decade. Plant Biotechnol. J. **20**, 256–282 (2022).

13. Liu, Y., Jafari, F. & Wang, H. Integration of light and hormone signaling pathways in the regulation of plant shade avoidance syndrome. aBIOTECH **2**, 131–145 (2021).

14. Huber, M., Nieuwendijk, N. M., Pantazopoulou, C. K. & Pierik, R. Light signalling shapes plant-plant interactions in dense canopies. Plant Cell Environ. **44**, 1014–1029 (2021).

15. Pedmale, U. V. et al. Cryptochromes interact directly with PIFs to control plant growth in limiting blue light. Cell **164**, 233–245 (2016).

16. Lorrain, S., Allen, T., Duek, P. D., Whitelam, G. C. & Fankhauser, C. Phytochrome-mediated inhibition of shade avoidance involves degradation of growth-promoting bHLH transcription factors. Plant J. **53**, 312–323 (2008).

17. Fernandez-Milmanda, G. L. & Ballare, C. L. Shade avoidance: expanding the color and hormone palette. Trends Plant Sci. **26**, 509–523 (2021).

18. Lin, X. et al. Novel and multifaceted regulations of photoperiodic flowering by phytochrome A in soybean. Proc. Natl Acad. Sci. USA **119**, e2208708119 (2022).

19. Song, Y. et al. Age-triggered and dark-induced leaf senescence require the bHLH transcription factors PIF3, 4, and 5. Mol. Plant **7**, 1776–1787 (2014).

20. Li, Z., Peng, J., Wen, X. & Guo, H. Ethylene-insensitive3 is a senescence-associated gene that accelerates age-dependent leaf senescence by directly repressing miR164 transcription in Arabidopsis. Plant Cell **25**, 3311–3328 (2013).

21. Sakuraba, Y. et al. Phytochrome-interacting transcription factors PIF4 and PIF5 induce leaf senescence in Arabidopsis. Nat. Commun. **5**, 4636 (2014).

22. Kim, C. et al. High ambient temperature accelerates leaf senescence via PHYTOCHROME-INTERACTING FACTOR 4 and 5 in Arabidopsis. Mol. Cells **43**, 645–661 (2020).

23. Casal, J. J. & Fankhauser, C. Shade avoidance in the context of climate change. Plant Physiol. **191**, 1475–1491 (2023).

24. Rivas-San Vicente, M. & Plasencia, J. Salicylic acid beyond defence: its role in plant growth and development. J. Exp. Bot. **62**, 3321–3338 (2011).

25. Richmond, A. E. & Lang, A. Effect of kinetin on protein content and survival of detached xanthium leaves. Science **125**, 650 (1957).

26. Abeles, F. B. et al. Induction of 33-kD and 60-kD peroxidases during ethylene-induced senescence of cucumber cotyledons. Plant Physiol. **87**, 609–615 (1988).

27. Chen, K. et al. Abscisic acid dynamics, signaling, and functions in plants. J. Integr. Plant Biol. **62**, 25–54 (2020).

28. Nohales, M. A. & Kay, S. A. GIGANTEA gates gibberellin signaling through stabilization of the DELLA proteins in Arabidopsis. Proc. Natl Acad. Sci. USA **116**, 21893–21899 (2019).

29. Sun, T. P. Gibberellin metabolism, perception and signaling pathways in Arabidopsis. Arabidopsis Book **6**, e0103 (2008).

30. Wen, C. K. & Chang, C. Arabidopsis RGL1 encodes a negative regulator of gibberellin responses. Plant Cell **14**, 87–100 (2002).

31. Sun, T. P. The molecular mechanism and evolution of the GA-GID1-DELLA signaling module in plants. Curr. Biol. **21**, R338–R345 (2011).

32. Chen, M. et al. Removal of DELLA repression promotes leaf senescence in Arabidopsis. Plant Sci. **219-220**, 26–34 (2014).

33. Zhang, Y. et al. DELLA proteins negatively regulate dark-induced senescence and chlorophyll degradation in Arabidopsis through interaction with the transcription factor WRKY6. Plant Cell Rep. **37**, 981–992 (2018).

34. Chen, L., Xiang, S., Chen, Y., Li, D. & Yu, D. Arabidopsis WRKY45 Interacts with the DELLA Protein RGL1 to Positively Regulate Age-Triggered Leaf Senescence. Mol. Plant **10**, 1174–1189 (2017).

35. Zhou, X., Jiang, Y. & Yu, D. WRKY22 transcription factor mediates dark-induced leaf senescence in Arabidopsis. Mol. Cells **31**, 303–313 (2011).

36. Zou, X., Seemann, J. R., Neuman, D. & Shen, Q. J. A WRKY gene from creosote bush encodes an activator of the abscisic acid signaling pathway. J. Biol. Chem. **279**, 55770–55779 (2004).

37. Johnson, C. S., Kolevski, B. & Smyth, D. R. TRANSPARENT TESTA GLABRA2, a trichome and seed coat development gene of Arabidopsis, encodes a WRKY transcription factor. Plant Cell **14**, 1359–1375 (2002).

38. Robatzek, S. & Somssich, I. E. Targets of AtWRKY6 regulation during plant senescence and pathogen defense. Genes Dev. **16**, 1139–1149 (2002).

39. Guo, P. et al. A tripartite amplification loop involving the transcription factor WRKY75, salicylic acid, and reactive oxygen species accelerates leaf senescence. Plant Cell **29**, 2854–2870 (2017).

40. Tian, T. et al. Arabidopsis FAR-RED ELONGATED HYPOCOTYL3 integrates age and light signals to negatively regulate leaf senescence. Plant Cell **32**, 1574–1588 (2020).

41. Liu, H. et al. Photoexcited CRY2 interacts with CIB1 to regulate transcription and floral initiation in Arabidopsis. Science **322**, 1535–1539 (2008).

42. Guo, H., Yang, H., Mockler, T. C. & Lin, C. Regulation of flowering time by Arabidopsis photoreceptors. Science **279**, 1360–1363 (1998).

43. Meng, Y., Li, H., Wang, Q., Liu, B. & Lin, C. Blue light-dependent interaction between cryptochrome2 and CIB1 regulates transcription and leaf senescence in soybean. Plant Cell **25**, 4405–4420 (2013).

44. Lyu, X. et al. GmCRY1s modulate gibberellin metabolism to regulate soybean shade avoidance in response to reduced blue light. Mol. Plant **14**, 298–314 (2021).

45. Cheng, B. et al. Shade-tolerant soybean reduces yield loss by regulating its canopy structure and stem characteristics in the Maize-soybean strip intercropping system. Front. Plant Sci. **13**, 848893 (2022).

46. Green-Tracewicz, E., Page, E. R. & Swanton, C. J. Shade avoidance in soybean reduces branching and increases plant-to-plant variability in biomass and yield per plant. Weed Sci. **59**, 43–49 (2017).

47. Matsumura, H. et al. Molecular cloning and linkage mapping of cryptochrome multigene family in soybean. Plant Genome **2**, 271–281 (2009).

48. Wang, T. et al. Light-induced mobile factors from shoots regulate rhizobium-triggered soybean root nodulation. Science **374**, 65–71 (2021).

49. Kozuka, T., Oka, Y., Kohzuma, K. & Kusaba, M. Cryptochromes suppress leaf senescence in response to blue light in Arabidopsis. Plant Physiol. **191**, 2506–2518 (2023).

50. Brouwer, B., Gardeström, P. & Keech, O. In response to partial plant shading, the lack of phytochrome A does not directly induce leaf senescence but alters the fine-tuning of chlorophyll biosynthesis. J. Exp. Bot. **65**, 4037–4049 (2014).

51. Xu, P. et al. Blue light-dependent interactions of CRY1 with GID1 and DELLA proteins regulate gibberellin signaling and photomorphogenesis in Arabidopsis. Plant Cell **33**, 2375–2394 (2021).

52. Zhong, M. et al. The blue light receptor CRY1 interacts with GID1 and DELLA proteins to repress GA signaling during photomorphogenesis in Arabidopsis. Mol. Plant **14**, 1328–1342 (2021).

53. Yan, B. et al. The blue light receptor CRY1 interacts with GID1 and DELLA proteins to repress gibberellin signaling and plant growth. Plant Commun. **2**, 100245 (2021).

54. Holtkotte, X., Ponnu, J., Ahmad, M. & Hoecker, U. The blue light-induced interaction of cryptochrome 1 with COP1 requires SPA proteins during Arabidopsis light signaling. PLoS Genet **13**, e1007044 (2017).

55. Blanco-Touriñán, N. et al. COP1 destabilizes DELLA proteins in Arabidopsis. Proc. Natl Acad. Sci. USA **117**, 13792–13799 (2020).

56. de Oliveira, R. et al. CRYPTOCHROME 1a-mediated blue light perception regulates tomato seed germination via changes in hormonal balance and endosperm-degrading hydrolase dynamics. Planta **257**, 67 (2023).

57. Wu, X. Y., Kuai, B. K., Jia, J. Z. & Jing, H. C. Regulation of leaf senescence and crop genetic improvement. J. Integr. Plant Biol. **54**, 936–952 (2012).

58. Luquez, V. M. & Guiamét, J. J. Effects of the 'stay green' genotype GGd1d1d2d2 on leaf gas exchange, dry matter accumulation and seed yield in soybean (Glycine max L. Merr.). Ann. Bot. **87**, 313–318 (2001).

59. Wang, P., Hou, S. Y., Wen, H. W., Wang, Q. Z. & Li, G. Q. Chlorophyll retention caused by STAY-GREEN (SGR) gene mutation enhances photosynthetic efficiency and yield in soybean hybrid Z1. Photosynthetica **59**, 37–Z48 (2021).

60. Keller, M. M. et al. Cryptochrome 1 and phytochrome B control shade-avoidance responses in Arabidopsis via partially independent hormonal cascades. Plant J. **67**, 195–207 (2011).

61. Earley, K. W. et al. Gateway-compatible vectors for plant functional genomics and proteomics. Plant J. **45**, 616–629 (2006).

62. Naito, Y., Hino, K., Bono, H. & Ui-Tei, K. CRISPRdirect: software for designing CRISPR/Cas guide RNA with reduced off-target sites. Bioinformatics **31**, 1120–1123 (2015).

63. Sun, X. et al. Targeted mutagenesis in soybean using the CRISPR-Cas9 system. Sci. Rep. **5**, 10342 (2015).

64. Paz, M. M., Martinez, J. C., Kalvig, A. B., Fonger, T. M. & Wang, K. Improved cotyledonary node method using an alternative explant derived from mature seed for efficient Agrobacterium-mediated soybean transformation. Plant Cell Rep. **25**, 206–213 (2006).

65. Hellens, R. P. et al. Transient expression vectors for functional genomics, quantification of promoter activity and RNA silencing in plants. Plant Methods **1**, 13 (2005).

66. Yoo, S. D., Cho, Y. H. & Sheen, J. Arabidopsis mesophyll protoplasts: a versatile cell system for transient gene expression analysis. Nat. Protoc. **2**, 1565–1572 (2007).

67. Yuan, Z. et al. Optimal leaf positions for SPAD meter measurement in rice. Front Plant Sci. **7**, 719 (2016).

68. Ying, Y. et al. Two h-type thioredoxins interact with the E2 ubiquitin conjugase PHO2 to fine-tune phosphate homeostasis in rice. Plant Physiol. **173**, 812–824 (2016).

69. Kereszt, A. et al. Agrobacterium rhizogenes-mediated transformation of soybean to study root biology. Nat. Protoc. **2**, 948–952 (2007).

70. Zhang, W. & Sun, Z. Random local neighbor joining: a new method for reconstructing phylogenetic trees. Mol. Phylogenet Evol. **47**, 117–128 (2008).

71. Bu, T. et al. A critical role of the soybean evening complex in the control of photoperiod sensitivity and adaptation. Proc. Natl Acad. Sci. USA **118**, e2010241118 (2021).

72. Xiong, L. et al. A transient expression system in soybean mesophyll protoplasts reveals the formation of cytoplasmic GmCRY1 photobody-like structures. Sci. China Life Sci. **62**, 1070–1077 (2019).

Acknowledgements

Author contributions
B.L. designed the research. Z.L., X.G.L., H.Y.L., Q.C.T., T.Z., and J.L. performed the experiments. Z.L., X.G.L., and H.Y.L. collected the phenotypic data. Z.L., X.G.L., and H.Y.L. analyzed data. B.L. and Z.L. wrote the manuscript.

Competing interests
The authors declare no competing interests.

Additional information
Supplementary information The online version contains supplementary material available at https://doi.org/10.1038/s41467-024-45086-5.

Correspondence and requests for materials should be addressed to Bin Liu.

Peer review information Nature Communications thanks Jorge Casal and Xin Zhou for their contribution to the peer review of this work. A peer review file is available.

Reprints and permissions information is available at http://www.nature.com/reprints

Publisher's note Springer Nature remains neutral with regard to jurisdictional claims in published maps and institutional affiliations.